SINTEF
PROCEEDINGS
2

Proceedings of the 12th International Conference on Computational Fluid Dynamics in the Oil & Gas, Metallurgical and Process Industries

Progress in Applied CFD – CFD2017

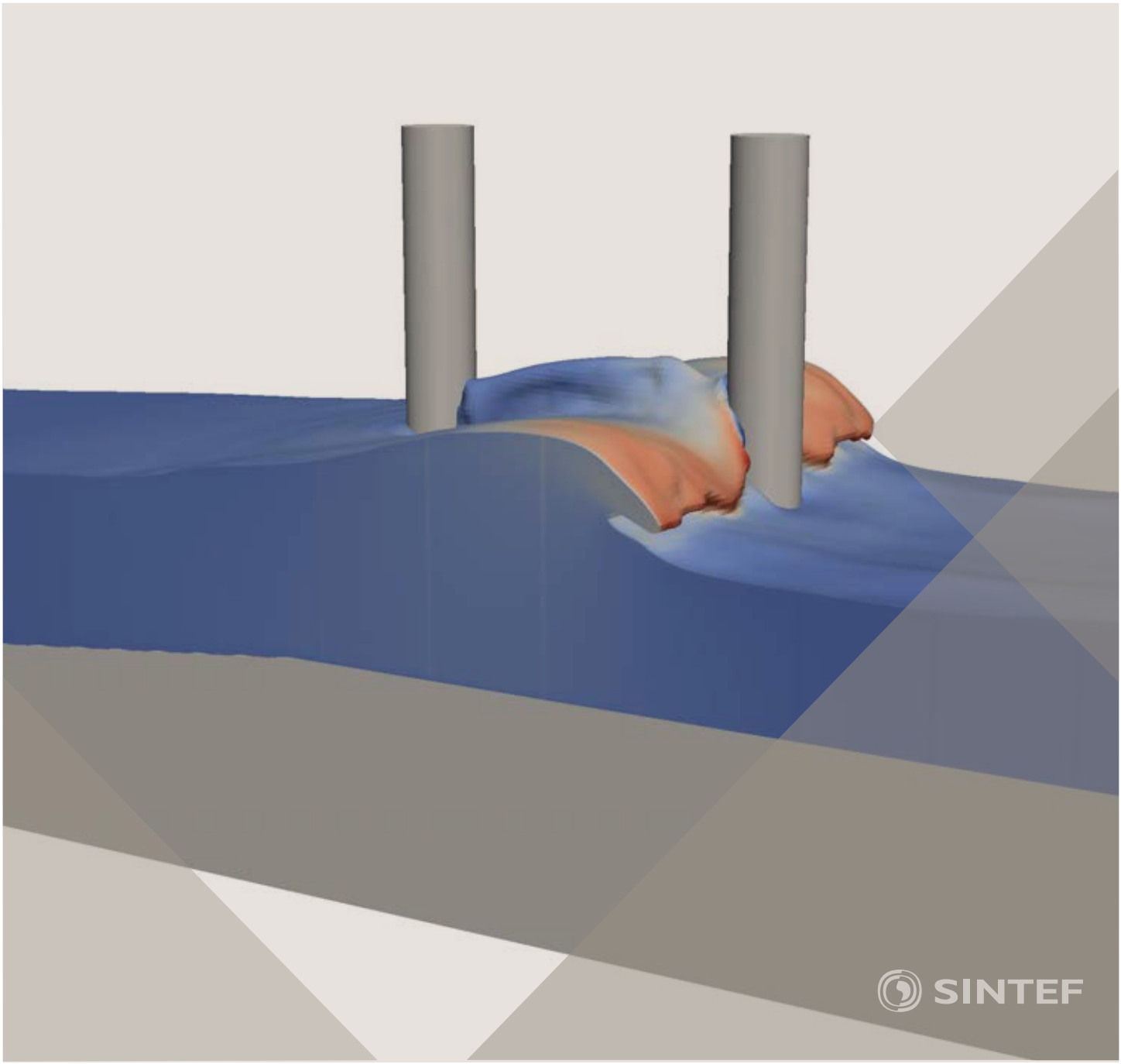

SINTEF Proceedings

Editors:
Jan Erik Olsen and Stein Tore Johansen

Progress in Applied CFD – CFD2017

Proceedings of the 12th International Conference on Computational Fluid Dynamics in the Oil & Gas, Metallurgical and Process Industries

SINTEF Academic Press

SINTEF Proceedings no 2
Editors: Jan Erik Olsen and Stein Tore Johansen
Progress in Applied CFD – CFD2017
Selected papers from 10th International Conference on Computational Fluid Dynamics in the Oil & Gas, Metallurgical and Process Industries

Key words:
CFD, Flow, Modelling

Cover, illustration: Arun Kamath

ISSN 2387-4295 (online)
ISBN 978-82-536-1544-8 (pdf)

SINTEF Academic Press
Address: Forskningsveien 3 B
PO Box 124 Blindern
N-0314 OSLO
Tel: +47 73 59 30 00
Fax: +47 22 96 55 08

www.sintef.no/byggforsk
www.sintefbok.no

SINTEF Proceedings
SINTEF Proceedings is a serial publication for peer-reviewed conference proceedings on a variety of scientific topics.
The processes of peer-reviewing of papers published in SINTEF Proceedings are administered by the conference organizers and proceedings editors. Detailed procedures will vary according to custom and practice in each scientific community.

PREFACE

This book contains all manuscripts approved by the reviewers and the organizing committee of the 12th International Conference on Computational Fluid Dynamics in the Oil & Gas, Metallurgical and Process Industries. The conference was hosted by SINTEF in Trondheim in May/June 2017 and is also known as CFD2017 for short. The conference series was initiated by CSIRO and Phil Schwarz in 1997. So far the conference has been alternating between CSIRO in Melbourne and SINTEF in Trondheim. The conferences focuses on the application of CFD in the oil and gas industries, metal production, mineral processing, power generation, chemicals and other process industries. In addition pragmatic modelling concepts and bio-mechanical applications have become an important part of the conference. The papers in this book demonstrate the current progress in applied CFD.

The conference papers undergo a review process involving two experts. Only papers accepted by the reviewers are included in the proceedings. 108 contributions were presented at the conference together with six keynote presentations. A majority of these contributions are presented by their manuscript in this collection (a few were granted to present without an accompanying manuscript).

The organizing committee would like to thank everyone who has helped with review of manuscripts, all those who helped to promote the conference and all authors who have submitted scientific contributions. We are also grateful for the support from the conference sponsors: ANSYS, SFI Metal Production and NanoSim.

Stein Tore Johansen & Jan Erik Olsen

Organizing committee:

Conference chairman: Prof. Stein Tore Johansen
Conference coordinator: Dr. Jan Erik Olsen
Dr. Bernhard Müller
Dr.Sigrid Karstad Dahl
Dr.Shahriar Amini
Dr.Ernst Meese
Dr.Josip Zoric
Dr.Jannike Solsvik
Dr.Peter Witt

Scientific committee:

Stein Tore Johansen, SINTEF/NTNU
Bernhard Müller, NTNU
Phil Schwarz, CSIRO
Akio Tomiyama, Kobe University
Hans Kuipers, Eindhoven University of Technology
Jinghai Li, Chinese Academy of Science
Markus Braun, Ansys
Simon Lo, CD-adapco
Patrick Segers, Universiteit Gent
Jiyuan Tu, RMIT
Jos Derksen, University of Aberdeen
Dmitry Eskin, Schlumberger-Doll Research
Pär Jönsson, KTH
Stefan Pirker, Johannes Kepler University
Josip Zoric, SINTEF

CONTENTS

NUMERICAL EVALUATION OF CO-FIRING SOLID RECOVERED FUEL WITH PETROLEUM COKE IN A CEMENT ROTARY KILN - EFFECT OF FUEL MOISTURE

David Jayanth ISAAC[1]*, Morten Nedergaard PEDERSEN[3], Damien GRÉVAIN[2], Lars Skaarup JENSEN[2], and Mads NIELSEN[2]

[1] FLSmidth Private Limited, 34, Egatoor, Kelambakkam, India

[2] FLSmidth A/S, Vigerslev Allé 77, DK-2500 Valby, Copenhagen, Denmark

[3] Technical University of Denmark, DK-2800 Lyngby, Denmark

*E-mail: david.jayanth@flsmidth.com

ABSTRACT

This paper presents a numerical simulation model for co-combustion of coarse Solid Recovered Fuel (SRF) with pulverised petroleum coke in a rotary kiln producing cement clinker. The objective is to derive a reliable modelling methodology for design and optimisation of a kiln burner and for the control of the co-combustion process. In this simulation model both the solid fuels are treated as dispersed phases using the Lagrangian method. Two separate shape factors are used to account for the thermodynamic and aerodynamic behaviour of the coarse irregular-shaped SRF particles. Both the fuels undergo similar combustion process - heating, drying, devolatilisation followed by volatile and char combustion. Using such a numerical model the influence of fuel moisture on ignition, flame intensity, fuel burnout and heat output is evaluated. Further insight into the behaviour of SRF particles and the flame characteristics are obtained from video images of the combustion process recorded at a cement plant.

Keywords: Multi-Fuel Burner, Rotary Cement Kiln, Co-firing, SRF, Fuel Moisture, Combustion Modelling.

NOMENCLATURE

Greek Symbols

ρ Density, [kg/m^3].
τ Stress tensor, [N/m^2].
λ Thermal conductivity, [W/m.K].
Γ Diffusion coefficient, [m^2/s].
Φ Reaction rate, [kg/m^3.s].

Latin Symbols

A Pre-exponential factor.
CS Cross-section area, [m^2].
D Kiln diameter, [m].
D_{eq} Equivalent diameter of spherical particle, [m].
Ea Activation energy, [kcal/mol].
g Acceleration due to gravity, [m/s^2].
h_t Total enthalpy, [m^2/s^2].
k Reaction rate constant.
p Static pressure, [Pa].
R Universal gas constant, [J/mol K].
SA Cross-section area, [m^2].
T Temperature, [K].
T_a Activation temperature, [K].
$\mathbf{u}$ Velocity, [m/s].
V Volume of particles, [m^3].
Y_i Mass fraction of species i.
z Axial distance inside the kiln, [m].

INTRODUCTION

In the cement industry rotary kilns are widely used for the production of cement clinker. This process is energy intensive and requires large quantities of fuels. Coal and other fossil fuels have traditionally been used as fuels in cement kilns. Driven by incentives to lower energy costs and waste co-processing, many cement companies increasingly substitute conventional fossil fuels such as coal, oil and natural gas with alternate fuels derived from waste. Solid Recovered Fuel (SRF) is one such alternative and is a solid fuel prepared from non-hazardous waste materials intended for firing in industrial furnaces. SRF consists of large amount of combustible materials like biomass and plastic. While it is attractive to substitute conventional fuels with biomass based fuels in economic and environmental terms, there are some characteristics of these fuels that can impact the kiln process adversely, and may for example reduce clinker quality and production rate.

A modern kiln burner must often be able to perform with high degree of SRF substitution. Hence it is vital to recognize the impacts of burning such alternate fuels in order to design and optimize the kiln combustion system. Irregular particle shape, inhomogeneous nature, high moisture content and prevention of unburnt SRF particle from reaching the clinker bed, while still maintaining a stable combustion, are some of the challenges to be overcome by an optimal burner design. Numerical simulations, with appropriate models for SRF combustion incorporated, is a useful tool for the control and investigation of the combustion process. It is possible to simulate in advance different co-firing concepts and scenarios giving valuable inputs to burner designers and kiln operators.

A number of studies have dealt with CFD simulations of the combustion of pulverized coal in cement kilns [1–4], but only a few papers have studied the effect of alternative fuels. Ariyaratne et al. [5] used CFD to compare the co-combustion of coal, meat and bone meal in the cement kiln, and Liedmann et al. [6] simulated the co-firing of lignite and SRF. Both studies found that the use of alternative fuels resulted in a lower gas phase temperature, due to an increased conversion time of the relatively large alternative fuel particles with high moisture content. A number of studies have also described CFD modelling and impact of SRF co-firing in cement calciners [7] and in power plants [8, 9]. The current study focuses on CFD modelling of co-firing SRF with petroleum coke in a cement rotary kiln.

CEMENT ROTARY KILN

A rotary kiln is a pyro processing device used to raise materials to a high temperature to enable clinker formation reactions in a cement plant. Figure 1 shows a rotary kiln positioned between the preheater tower and the clinker cooler.

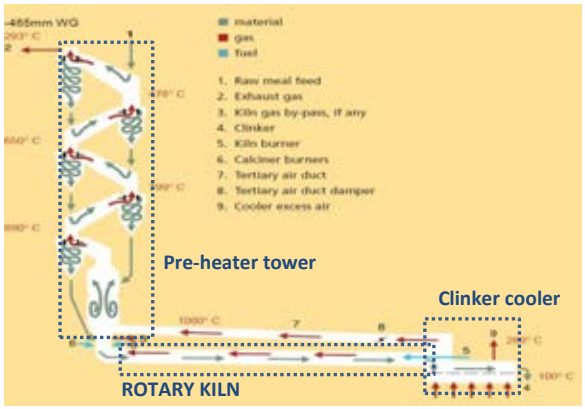

Figure 1: Schematic of a modern cement kiln system

The kiln is a long, cylindrical tube consisting of an outer steel shell and an inner refractory lining. In the material outlet end the kiln is equipped with a burner. The main function of the burner is to form a flame to provide energy for clinkerisation. The flame should be short, narrow and strongly radiant in order to achieve a good heat transfer from the flame to the materials in the bed.

The burner fires the kiln with pulverized coal or coke, oil, natural gas or even as in this case secondary fuels such as plastic chips, wood chips, paper, packing material, etc. Most of the air required for combustion is the hot secondary air from the cooler entrained into the fuel jet and the rest is cold primary air introduced through the burner. The primary air is further divided into multiple channels to impart axial and tangential momentum which helps in controlling the flame shape and also to assist in fuel conveying and cooling the burner tip.

COMPUTATIONAL METHOD

The modelling method is based upon the solution of the equations governing compressible fluid flow on a finite volume mesh representing the inside of a kiln with a burner, as illustrated in Figure 2. The commercial CFD software ANSYS CFX, was used for modelling and simulation of the combustion process. The governing equations of conservation of mass, momentum, energy and species mass fraction in the continuous gas phase is described in equations 1 to 4.

$$\frac{\partial \rho}{\partial t} + \nabla \cdot (\rho \mathbf{u}) = S_m \quad (1)$$

$$\frac{\partial (\rho \mathbf{u})}{\partial t} + \nabla \cdot (\rho \mathbf{u}\mathbf{u}) = -\nabla p + \nabla \cdot (\tau) + \rho g + F \quad (2)$$

$$\frac{\partial (\rho h_t)}{\partial t} - \frac{\partial (p)}{\partial t} + \nabla \cdot (\rho \mathbf{u} h_t) = \nabla \cdot (\lambda \nabla T) + \nabla \cdot (\mathbf{u} \cdot \tau) + S_e \quad (3)$$

$$\frac{\partial (\rho Y_i)}{\partial t} + \nabla \cdot (\rho \mathbf{u} Y_i) = \nabla \cdot (\rho \Gamma_i \nabla Y_i) + \Phi_i \quad (4)$$

Here, S_m is the mass source added to the continuous phase (due to evaporation, devolatilisation and char reaction); F is the external body force that arises due to interaction with the dispersed phase; Se represents the heat source due to combustion; Γ is the diffusion coefficient of species i and Φ is the reaction rate. In addition the two equation model of Shear Stress Transport (SST) is used to predict turbulence, as the flow has moderate swirl generated by the burner. Heat transfer by radiation is computed using the discrete transfer radiation model.

The finite volume mesh must be adequate to capture the presence of a large range of length scales that needs to be resolved, ranging from the dimensions of individual primary air nozzles (hydraulic diameter ≈25 mm) to the overall size of the kiln (diameter=5m; length=75 m).

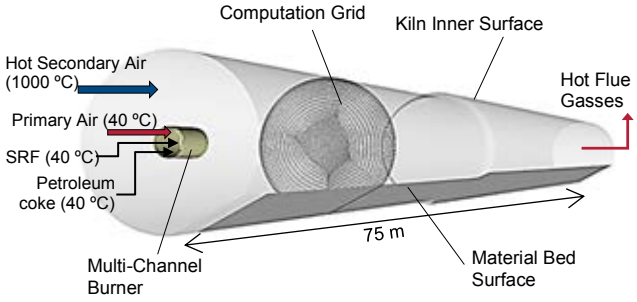

Figure 2: Computation domain and boundary conditions

All the gas and particle inflow boundaries are defined by specified mass flow rate and temperature, while the outlet has a defined pressure.

In this simulation model the actual process of clinkerisation is not modeled instead a predefined temperature profile (Figure 3) is applied to the inner walls of kiln and the material bed thereby representing the surfaces from which heat is transferred to and from the flame or process gasses.

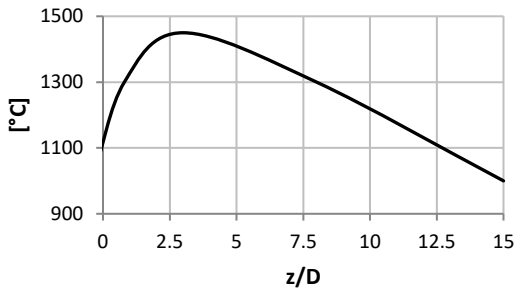

Figure 3: Predefined material bed surface and kiln wall temperature [1] applied in the computational method

The two fuels, petroleum coke and SRF, are tracked using the Lagrangian particle transport model. Petroleum coke is a conventional fuel and is ground to a fine degree to be completely burnt in the kiln. The particle size distribution of petroleum coke is represented in figure 4. A Rosin-Rammler distribution is fitted to the PSD data and is used to model injection of petroleum coke particles.

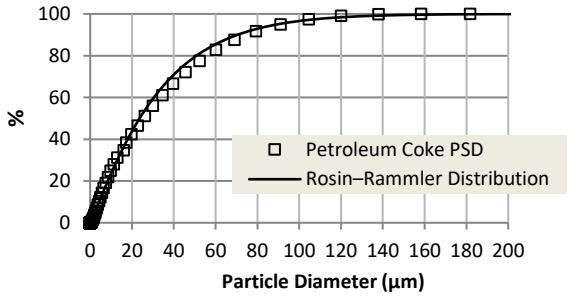

Figure 4: Cumulative particle size distribution of petroleum coke

SRF on the other hand, is coarse and has an irregular shape, mostly flat 2D foils of paper, cardboard, packing material and plastics [6 and 11]. For the purpose of modelling all SRF particles are considered to be flat particles of size 10mm wide, 20mm long and 0.1mm thick. Each flat particle is represented by a spherical particle with an equivalent diameter computed based on volume (Figure 5).

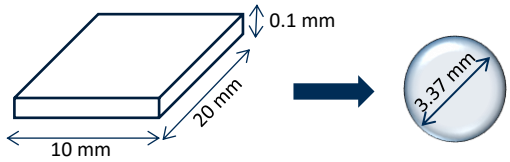

Figure 5: Representation of flat SRF particle as a sphere

Equivalent diameter of spherical particle

$$D_{eq} = \sqrt[3]{\frac{6 \times V}{\pi}} \tag{5}$$

The coarse irregular-shaped SRF particles are specially treated with shape factors to account for variations in thermodynamic behaviour and aerodynamic behaviour (Parameter values summarised in Table 1).

The Cross Sectional Area Factor (CSAF) is included to account for the influence of drag force of a non-spherical particle on the assumed spherical particle.

$$CSAF = \frac{CS}{\pi\left(\frac{D_{eq}}{2}\right)^2} \tag{6}$$

Similarly the Surface Area Factor (SAF) is applied to account for mass and heat transfer correlations of a non-spherical particle on a spherical particle. It is defined as the ratio of the actual surface area to the surface area of a spherical particle with the same equivalent diameter:

$$SAF = \frac{SA_{\text{cuboidal}}}{SA_{\text{sphere}}} \tag{7}$$

Table 1: SRF particle size and shape factors used in the simulations.

	Units	Value
Flat Particle		
Width	*mm*	*10*
Length	*mm*	*20*
Thickness	*mm*	0.1
Volume (V)	mm^3	20
Cross Section Area (CS)	mm^2	200
Surface Area (SA)	mm^2	406
Equivalent Spherical Particle		
Diameter (D_{eq})	*mm*	*3.37*
Surface Area (SA)	mm^2	*35.63*
Surface Area Factor (SAF)		*11.39*
Cross Sectional Area Factor (CSAF)		*22.45*

Combustion of both the solid fuels is divided into four stages: heating, drying, devolatilisation followed by volatile and char combustion. These stages are illustrated in figure 6.

After initial heating to approximately 100ºC, moisture is evaporated and transported away from the particles:

$$H_2O_{(l)} \rightarrow H_2O_{(g)} \tag{8}$$

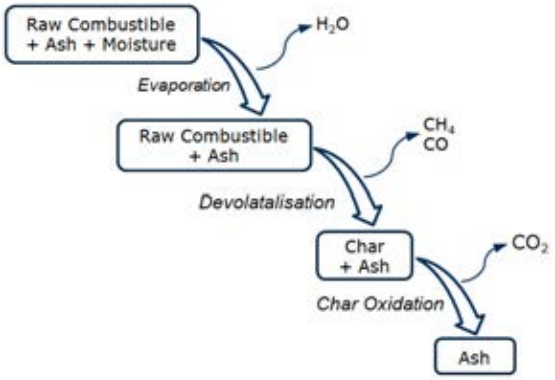

Figure 6: Stages of solid fuel combustion

The next step is devolatilisation, which is the release of volatiles into the gas stream. The process is initiated by external heating when the particle surface temperature reaches the lower devolatilisation temperature. This is an endothermic reaction absorbing heat from the surrounding environment. In the current study the volatile gas is assumed to consist of only CH_4 and CO. The distribution of CH_4 and CO in volatiles is adjusted such that the total energy in the fuel is balanced:

$$\begin{pmatrix}\text{Energyin Volatiles}\\(CH_4 + CO)\end{pmatrix} = \begin{pmatrix}\text{Energyin}\\\text{Raw Combustible}\end{pmatrix} - \begin{pmatrix}\text{Energyin}\\\text{Char}\end{pmatrix} \quad (9)$$

In an oxygen environment the devolatilised products ignite in a flame front, above the outer surface and undergo volatile oxidation, enhancing heat transfer to the surface. This accelerates the overall devolatilisation process. A two-step process defined by Westbrook Dryer WD2 [10] is considered to define homogenous volatile oxidation:

$$CH_4 + 1.5O_2 \rightarrow CO + 2H_2O \quad (10)$$

$$CO + 0.5O_2 \rightarrow CO_2 \quad (11)$$

The final step is char combustion where the remaining fuel particle consisting almost entirely of carbon and ash is converted into ash. During the char conversion process, oxygen is transported from the surrounding gas to the solid fuel outer surface and eventually into the porous surfaces by diffusion, where it reacts with solid carbon to release carbon dioxide.

$$C_{(s)} + O_2 \rightarrow CO_2 \quad (12)$$

All the reactions including evaporation are modelled using a kinetic approach with an Arrhenius type equation. The dependence of the rate constant k of the chemical reactions on the temperature T and activation energy E_a is computed as shown in equation 13.

$$k = A \times e^{-\left(\frac{T_a}{T}\right)} \text{ (or) } k = A \times e^{-\left(\frac{E_a}{RT}\right)} \quad (13)$$

Table 2: Adopted kinetics for multiphase reactions

	Units	Pet coke[12]	SRF[11]
Evaporation			
Pre-exp. factor (A)	s^{-1}	1.00E+10	1.00E+10
Activation Temperature (T_a)	*K*	9273	9273
Devolatilisation			
Pre-exp. factor (A)	s^{-1}	1.05E+13	3.01E+16
Activation Temperature (T_a)	*K*	25227	26110
Char Oxidation			
Pre-exp. factor (A)	$g/cm^2\ s$	7	5.69E+08
Activation Energy (E_a)	*kcal/mol*	19.7	35.80

Evaporation, devolatilisation and char oxidation are multiphase reactions involving solid and gaseous phases. Whereas the volatile oxidation is a homogenous reaction where all the reactants and products are in gaseous phase. Table 2 and 3 summarises the kinetic parameters used in the model.

Table 3: Adopted kinetics for volatile oxidation [10]

	Units	
Methane oxidation		
Pre-exp. factor (A)	s^{-1}	1.5E+07
Activation Energy (E_a)	*kcal/mol*	30
CO oxidation		
Pre-exp. factor (A)	$m^{2.25}\ s^{-1}\ mol^{-0.750}$	1.26e+10
Activation Energy (E_a)	*kcal/mol*	40

SIMULATED CONDITIONS AND RESULTS

This CFD modelling study examines the effect of moisture in SRF, when co-firing with pulverized petroleum coke, on flame intensity, fuel burnout and heat output. Moisture content in the fuel is an important issue to consider when burning SRF in kilns. During operation the burner can receive SRFs with varying degree of moisture. The heating value of the fuel decreases with increased moisture content. High moisture content will reduce the combustion temperature, hindering the amount of heat transferred to the material bed resulting in poor quality of clinker. In such an event the operator will increase the rate of fuel flow or reduce the substitution rate to maintain the combustion temperature in the kiln.

Conditions for simulation represent co-firing at a substitution rate of 70% with SRF. Substitution rate here refers to the amount of conventional fuel substituted by secondary fuels like SRF, calculated based on the burner's thermal output. Three grades of SRF are considered for this study with varying amounts of moisture in the fuel. The ultimate and proximate analysis of these three SRFs and petroleum coke is summarised in table 4.

Table 4: Proximate and Ultimate analysis

	Pet coke	SRF10	SRF20	SRF40
Proximate (% wt as received)				
Moisture	0.52	10.00	20.00	40.00
Volatiles	12.94	64.35	57.20	42.90
Fixed Carbon	77.48	6.89	6.12	4.69
Ash	9.07	18.77	16.68	12.51
Ultimate (% wt as received)				
C	82.46	47.05	41.82	31.37
H	3.84	6.68	5.94	4.46
N	2.15	0.38	0.34	0.26
O	0.43	16.52	14.68	11.01
S	1.54	0.08	0.07	0.05
Cl	0.00	0.53	0.47	0.35
Net Calorific Value (MJ/kg)	32.7	20.14	17.62	12.69
Mass Flow Rate (kg/s)	0.56	2.13	2.43	3.40

With the increase in fuel moisture, the quantity of SRF fuel is increased to keep the burner's total thermal power output unchanged. The mass of primary air remains same in the three cases, thereby keeping the axial and swirl momentums from the burner constant. The amount of secondary air though is varied such that the equivalence ratio of the combustion system is maintained at 1.2 for all cases.

Petroleum coke enters the kiln through an annular channel in the burner, devolatilises and undergoes volatile combustion setting the ignition point of the flame. The high temperatures generated by combustion of petroleum coke, accelerates heating and drying of the coarse SRF particles which are injected through a separate circular central channel. The devolatilized gasses from SRF burn to complete the flame. Only 30% of the total burner power is derived from petroleum coke. Hence it attains almost complete combustion with very little unburnt char left, which are normally carried away with the flue gasses. On the contrary, the larger SRF particles fall to the material bed (Figure 7). These particles undergo partial char combustion while they are in suspension and the rest burns on the material bed when enough oxygen is available.

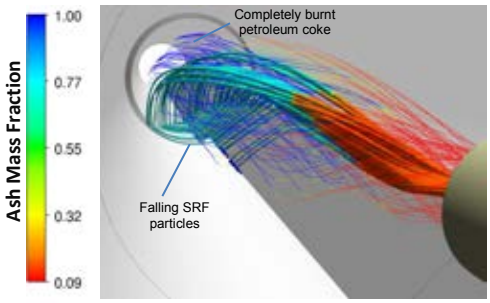

Figure 7: Particle tracks of SRF and petroleum coke

In this simulation the Lagrangian particles are no longer tracked after 200s. This time interval is sufficient for the particles to reach the material bed, but is not enough to ensure complete combustion of the char particles on the bed. Limiting the particle tracking time, leads to a fraction of the total heat energy to be unaccounted in the model. Fortunately this unaccounted heat, that is lost as unburnt char particles along with their sensible heat, is a good indication of the degree of fuel not burning while in suspension.

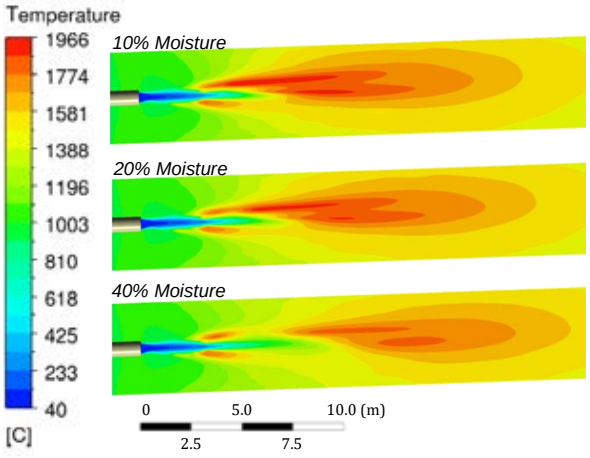

Figure 8: Temperature contours determined for the three SRF moisture contents

Tempratrure plots of flames produced in the three scenarios (shown in figure 8), reveal that when operating at 70% substitution, the influence of moisture is more felt when the fraction of moisture is very high. SRF with 10% and 20% moisture show little difference in flame shape, ignition and useful heat output. Ignition in all cases is controlled by the flame produced by burning of petroleum coke.

The SRF particles are heated to evaporation temperature, by the hot secondary air and by radiations from the walls. In the low moisture cases, rapid release of moisture happens in the vicinity of high temperatures generated by the petroleum coke flame (Figure 9). This initial flame provides enough heat to overcome the latent heat required for vaporisation and promote further heating of SRF particles to devolatalization temperature. In this scenario the petroleum coke flame and the SRF flame appear attached to each other.

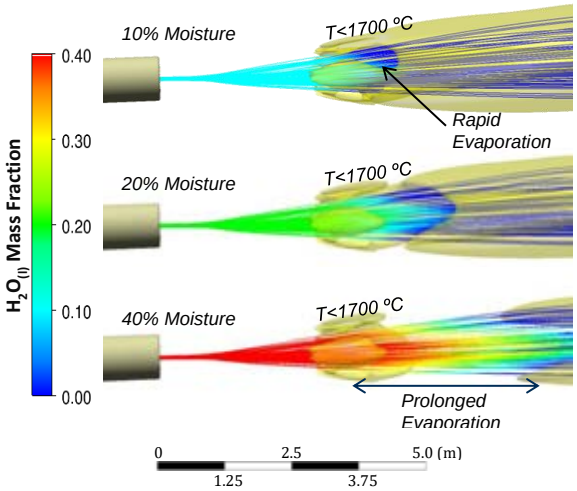

Figure 9: Particle tracks coloured with mass fraction of water

In the high moisture case, the particle heating and evaporation phase is prolonged. Moisture release happens outside the high temperature zone created by the combustion of petroluem coke. Under this condition, reduction in gas temperatures are observed in the near burner zone (z/D<2) (Figure 9 and 10) owing to a stretched evaporation phase, further delaying devolatilisation and volatile combustion. A gap develops between the flames from the two fuels.

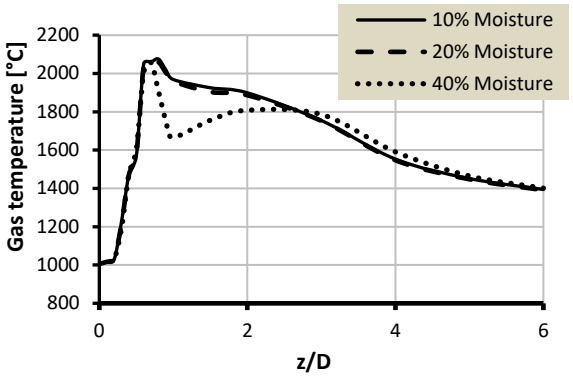

Figure 10: Peak gas temperatures in the burning zone plotted as a function of distance/diameter (z/D)

The comparison of the total distribution of heat among the three moisture cases is shown in figure 11. A big fraction of input heat (in the form of fuel firing) is available for clinkerisation. A portion is lost as unburnt carbon in char and the rest are the heat lost through the kiln shells and the heat carried away by the flue gasses.

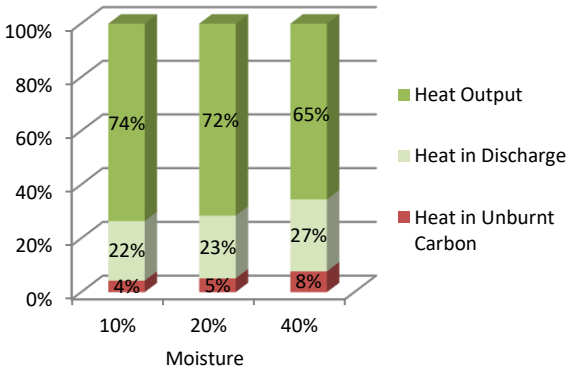

Figure 11: Heat distribution between: Bed and walls (Heat output); Gas stream leaving kiln (heat in discharge); and Unburnt fuel.

Heat available for clinkerisation is measured in each simulation as a heat flux on the material bed and the kiln walls. This is used as a parameter to evaluate the performance at different operating conditions. Figure 12 compares the cumulative heat transferred to the material surface and kiln walls for the three scenarios. The rate of heat transferred is rapid in the near burner flow field where most of the combustion occurs and is gradual in the regions away from the burner.

The amount of heat transferred in the burning zone (z/D<5) influences the process of clinkerisation. With 40% moisture in the fuel the cumulative heat flux in the burning zone reduces by 6MW.

Quite clearly the higher moisture content reduces the amount of heat available for clinkerisation even when the total burner power is maintained by firing additional quantities of fuel. The influence of moisture can be expected to become more significant when the substitution rate is further increased beyond 70%.

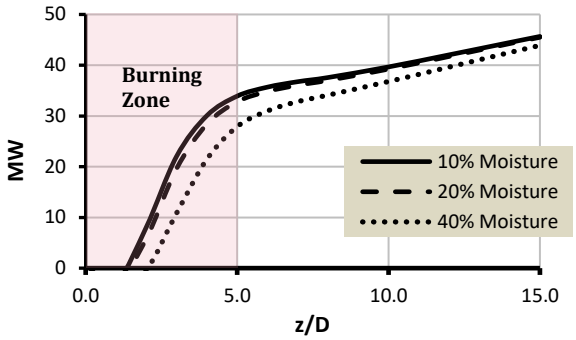

Figure 12: Cumulative heat flux on the walls and bed surface

INDUSTRIAL TESTS

It was also desirable to use industrial measurements to investigate the effect of different fuels and burner settings on the flame and also to derive input conditions for CFD simulations and to validate models. A number of measurements have been performed at a full-scale cement plant firing a mix of petroleum coke and SRF. A water-cooled camera probe was developed to obtain detailed video images of the combustion process in the cement kiln. This made it possible to insert a camera in the hot environment next to the kiln burner (Figure 13).

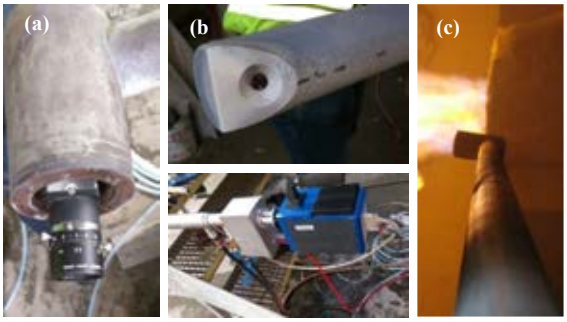

Figure 13: (a) Visual camera (b) infra-red camera and (c) video probe inserted into the kiln hood

The images are used to compare the differences in ignition point, flame shape, and fuel flow of a petroleum coke flame and a co-fired flame.

An example comparison is shown in figure 14. The petroleum coke flame (figure 14a) ignites earlier than the co-fired flame (figure 14b), which is due to a larger particle size of SRF and higher moisture content, that cools the flame. It is estimated that the ignition point is approx. 2-3 m from the burner tip when using petroleum coke, and that the ignition point is delayed 1 to 2 meter further when SRF is co-fired.

The petroleum coke flame plume is also wider due to the petroleum coke being added through an annular channel, where it can more readily expand than the SRF, which is added through a central pipe.

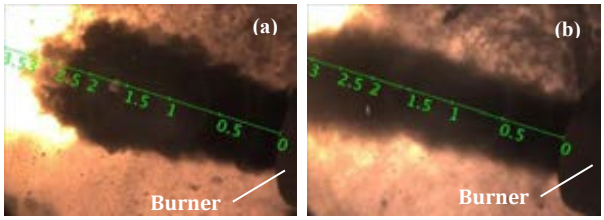

Figure 14: Images of a) Petroleum coke flame, b) co-fired flame (scale is in 'm')

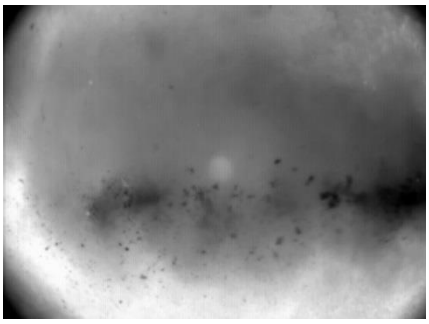

Figure 15: Images of co-fired flame with infrared camera.

The image in Figure 15 is recorded with the use of an infrared camera. This is well suited to track the flight behaviour of SRF particles inside the kiln. The SRF is shown as large dark particles in the IR image, which indicate a low particle temperature. The cold particles can be tracked relatively far inside the kiln, indicating a low conversion. This will likely result in some of the SRF particles landing in the kiln bed unconverted, as also indicated in the CFD simulations.

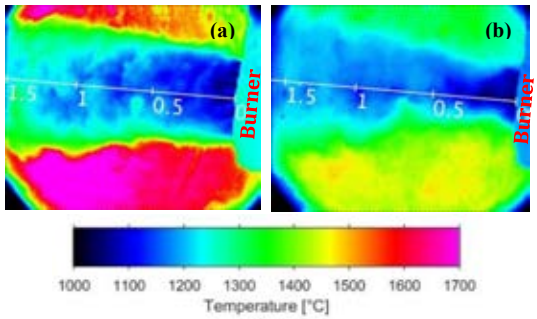

Figure 16: Temperature estimation (a) petroleum coke firing and (b) co-firing with SRF, (scale is in 'm')

The infrared camera was calibrated using a black body inserted in an oven, to get a relationship between the temperature of the unit and the camera image intensity. This allows for an estimate of the temperature in the near burner zone constituting approximately the first 5 meters of the kiln. An example is shown in Figure 16 with the temperature of a petroleum coke flame (figure 16a) and the co-fired flame (figure 16b). The temperatures for the petroleum coke flame are significantly higher, with the highest temperature exceeding 1700 °C. For the co-fired flame the maximum temperature in the near burner zone is around 1500 °C.

CONCLUSIONS AND OUTLOOK

The presented work studies the influence of moisture in the fuel on combustion characteristics and useful heat output while co-firing a cement kiln with petroleum coke and SRF at 70% thermal substitution. The results give an overview of the capabilities of CFD in the field of combustion modelling of large sized secondary fuels typically burnt in the cement industry. An overview of the models that have to be considered is presented. Trends of the simulated results compare qualitatively with video recordings.

Focused analysis of the results provides a deeper insight into the physical and thermal behaviour of such fuels. Model predictions from CFD simulations can be further sharpened by proper assumptions of reaction rate of the char burnout reaction of SRF along with better definitions of the composition of the volatile gases, their formation during devolatilisation and combustion modelled with more complex reaction schemes. Such a model can be used further to understand the influence of different operating parameters and investigate different injection concepts to optimise burner designs.

REFERENCES

[1] WANG, S., LU, J., LI, W., LI, J., and HU, Z., (2006), "Modeling of Pulverized Coal Combustion in Cement Rotary Kiln", *Energy & Fuels 2006*, 20, 2350-2356.

[2] LOCKWOOD, F. C, and SHEN, B., (1994), "Performance predictions of pulverised-coal flames of power station furnace and cement kiln types", *Twenty-Fifth Symposium (International) on Combustion,* 1994, pp. 503–509.

[3] MASTORAKOS, E., MASSIAS, A., TSAKIROGLOU, C.D., GOUSSIS, D.A., BURGANOS, V.N., and PAYATAKES, A.C., (1999), "CFD predictions for cement kilns including flame modelling, heat transfer and clinker chemistry", *Applied Mathematical Modelling,* 1999, 23, 55–76.

[4] MUJUMDAR, K.S., and RANADE, V.V., (2008), "CFD modeling of rotary cement kilns", *Asia-Pacific Journal of Chemical Engineering*, 2008, 3, 106–118.

[5] ARIYARATNE, W.K.H., MALAGALAGE, A., MELAAEN, M.C., and TOKHEIM, L.-A., (2014), "CFD Modeling of Meat and Bone Meal Combustion in a Rotary Cement Kiln", International Journal of Modeling and Optimization, 2014, 4, 263–272.

[6] LIEDMANN, B., ARNOLD, W., WIRTZ, S., SCHERER, V., KRÜGER, B., MROTZEK, A., HÜNDGEN, W., and TOPP, O., (2015), "Refuse Derived Fuel Co-Firing in Cement Rotary Kilns – A methodology to specify a customized fuel by numerical simulation and fuel characterisation", *10th European Conference on Industrial Furnaces and Boilers*, 2015, pp. 1–11.

[7] NAKHAEI, M., WU, H., GLARBORG, P., DAM-JOHANSEN, K., GRÉVAIN, D., and JENSEN, L.S., (2016), "CFD simulation of a full-scale RDF-fired calciner", *Proceedings of the 2nd International Workshop on CFD and Biomass Thermochemical Conversion,* Leipzig, 9 September 2016.

[8] LIEDMANN, B., ARNOLD, W., KRÜGER, B., BECKER, A., KRUSCH, S., WIRTZ, S., and SCHERER, V., (2017), "An approach to model the thermal conversion and flight behaviour of Refuse Derived Fuel", *Fuel,* 2017, 200, 252–271.

[9] AGRANIOTIS, M., NIKOLOPOULOS, N., NIKOLOPOULOS, A., GRAMMELIS, P., and KAKARAS, E., (2010), "Numerical investigation of Solid Recovered Fuels' co-firing with brown coal in large scale boilers - Evaluation of different co-combustion modes", *Fuel*, 2010, 89, 3693–3709.

[10] WESTBROOK, C.K., DRYER, F.L., (1981), "Simplified Reaction Mechanisms for the Oxidation of Hydrocarbon Fuels in Flames", *Combustion Science and Technology,* 1981 Vol. 27, pp. 31-43.

[11] PEDERSEN, P.N., (2015), "Single particle combustion of refuse derived fuel", *Technical report, Technical University of Denmark,* Department of Chemical and Biochemical Engineering.

[12] SMITH, I. W., (1982), "The Combustion Rates Of Coal Chars: A Review", *Nineteenth Symposium (International) on Combustion/The Combustion Institute*, 1982/pp. 1045-1065.